Enhanced visible light photocatalytic performance of Cu/ZnO nanocomposites

JIE LIU, CHANGZHEN LIU*, RUI CHEN, XIAOXIANG FANG, LIN CONG[a], YONGQIAN WANG, XIAOHONG YU, XIULING WU*
Faculty of Materials Science and Chemistry, China University of Geosciences, Wuhan 430074, China
[a]*Library, Jilin Normal University, Siping 136000, China*

The Cu/ZnO nanocomposites with different Cu content of 20 wt%, 40 wt%, 60 wt% and 80 wt% were synthesized via chemical deposition method. The structure, morphology and optical properties of Cu/ZnO nanocomposites were characterized by X-ray diffraction, field emission scanning electron microscopy and ultraviolet-visible spectroscopy. The photocatalytic activity for degradation of methyl orange (MO) revealed that the Cu/ZnO nanocomposites have markedly improved visible light photocatalytic performance than the pure ZnO. The enhanced photocatalytic performance was correlated with the interface between ZnO and Cu nano particles. The ideal Cu content turned out to be 60 wt%.

(Received June 6, 2015; accepted August 3, 2016)

Keywords: Photocatalysis, Cu/ZnO nanocomposites, Chemical deposition, Interface

1. Introduction

Photocatalysis has attracted great interest in recent years due to its potential in solving many current environmental problems such as air and water pollution [1,2]. Among the commonly known photocatalysts, zinc oxide (ZnO) has received much attention due to its direct wide band gap (3.37 eV), high exaction binding energy (60 meV), physical and chemical stability and rarely low cost [3-5]. When under irradiation with energy larger than the bad gap of ZnO, the electrons in the valence band (VB) of ZnO will be excited to the conduction band (CB), and thus form electron-hole pairs [6-8]. The photo-induced electrons and holes are able to activate the surrounding chemical species and then promote the chemical reactions.

However, the rapid recombination of photo-induced hole-electron pairs and low photocatalytic efficacy under visible illumination are major obstacles for increasing photocatalytic efficiency of ZnO photocatalyst [9]. Therefore, many methods have been introduced by researchers as a useful tool to suppress the photo-excited electron-hole recombination and broaden the absorption spectra in order to improve the photocatalytic performance of ZnO [10-13]. Noble metals, such as Pt, Ag, and Au have been used in preparation of a series of complex heterostructure with ZnO for enhanced photochemical performance, which could help the charge transfer and inhibit the charge recombination by trapping the photo-induced charge and improve the photo-electrochemical performance of the semiconductor materials [14-17]. Because of the relatively high cost of noble metal, we try to use other non-noble metal in replacement without scarifying photocatalytic properties of ZnO.

Few researches have been reported about the Cu/ZnO nanocomposites. In the present study, we deposited elementary Cu on the surface of ZnO, and the effect of different Cu content on the structure, morphology, optical properties was discussed. Finally, the degradation of MO was used to value the photocatalytic performance of the samples.

2. Experimental

2.1 Materials

All chemicals were analytical grade and used as received without purification. Zinc acetate ($Zn(CH_3COO)_2{\cdot}2H_2O$), Oxalic acid ($C_2H_2O_4$), hexadecyltrimethyl ammonium bromide (CTAB), ethanol (C_2H_5OH), copper nitrate ($Cu(NO_3)_2{\cdot}3H_2O$), methyl orange (MO), hydrazine hydrate($N_2H_4{\cdot}2H_2O$), ammonium hydroxide ($NH_3{\cdot}H_2O$) were all purchased from Sinopharm Group Chemical Reagent Co. Ltd., China. Deionized water was used in all experiments.

2.2 Synthesis of pure ZnO

4.390g Zinc acetate ($Zn(CH_3COO)_2{\cdot}2H_2O$) was dissolved in 20 mL deionized water under vigorously stirring then 3g Oxalic acid ($C_2H_2O_4$) were introduced into the above solution under continuous stirring for 1.5 h. The precipitation was dried at 50 °C, and then roasted at 450°C,

and pure ZnO was obtained.

2.3 Synthesis of Cu/ZnO nanocomposites

3.802g copper nitrate ($Cu(NO_3)_2 \cdot 3H_2O$) was dissolved in 100 mL hexadecyltrimethyl ammonium bromide (CTAB) solution with the concentration of 0.01 mol/L, then adjusted pH to 10 with ammonium hydroxide ($NH_3 \cdot H_2O$). A series of ZnO under the mass mixing ratios of 20 wt%, 40 wt%, 60 wt% and 80 wt% were introduced into the solution under stirring for 0.5 h, and then solution A was obtained. 15.000 g ammonium hydroxide ($NH_3 \cdot H_2O$) was dissolved in another 100 mL hexadecyltrimethyl ammonium bromide (CTAB) solution, and solution B was obtained. Mixed solution B with solution A slowly under continuous stirring for 3 h at 50 °C, then the products were vacuum filtrated with C_2H_5OH and deionized water. Finally the products were dried at 50 °C and the Cu/ZnO nanocomposites were obtained.

2.4 Characterization

The structures of all the samples were characterized by X-ray diffraction (XRD) using a Dmax-3β diffractometer with nickel-filtered Cu Kα radiation. The surface morphologies of the Cu/ZnO nanocomposites were taken on a Hitachi SU8010 electron microscope (FE-SEM). And the UV-vis absorbance value was measured with a Shimadzu UV-2550 UV-Visible apparatus. The photocatalytic activity was valued by the degradation of MO (10 mg/L) solution. The concentration of catalyst in the solution is 0.1 g/L.

3. Results and discussion

3.1 Mechanism

Chose $Cu(NO_3)_2 \cdot 3H_2O$ as copper source and adjust the pH with $NH_3 \cdot H_2O$, then the metallic copper complex solution was obtained. When the N_2H_4 was introduced into the solution, Cu was deposited on the surface of ZnO.

$$2Cu(NH_3)_2^{2+} + N_2H_2 + 4OH^- \rightarrow 2Cu\downarrow + N_2\uparrow + 4\,NH_3 \cdot H_2O$$

3.2 Structure and morphology

The XRD patterns of the as-synthesized samples with different Cu content are shown in Fig. 1. Only hexagonal wurtzite ZnO (JCPDS No. 36-1451) was detected for the sample without Cu, while for other samples, face-centered-cubic (*fcc*) metallic Cu (JCPDS No. 85-1326) marked with "•" were also identified in addition to hexagonal ZnO. However, there is no remarkable shift of all diffraction peaks, implying that no $Zn_{1-x}Cu_xO$ solid solution was formed and the change of the lattice parameters of ZnO nanocrystalsis negligible. Furthermore, a consistent decrease in relatively intensity of ZnO peaks but an increase of Cu peaks can be noted with the increase in concentration of Cu.

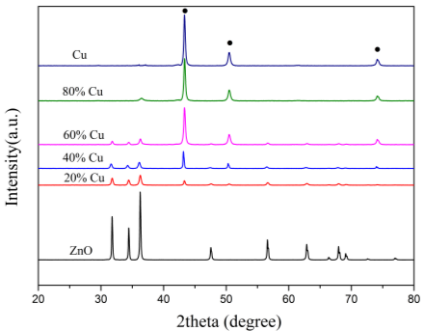

Fig. 1. XRD patterns of as-synthesized samples with different Cu content

Fig. 2 (a) shows the FE-SEM images of pure ZnO, it can be seen that the nanospindles consist of smaller nanoparticles. Fig. 2 (b and c) show the FESEM images of Cu nanoparticle decorated ZnO nanospindles prepared using different concentrations of Cu^{2+}. It's clear that with the increase of Cu concentration, there is increased aggregation of the nanoparticles into nanospindles of complex morphology. Obvious agglomeration was observed for the pure Cu as shown in Fig. 2 (d). The presence of small nanoparticles modifies the surface of these ZnO nanospindles and the complex aggregated nanospindle structures can be clearly seen.

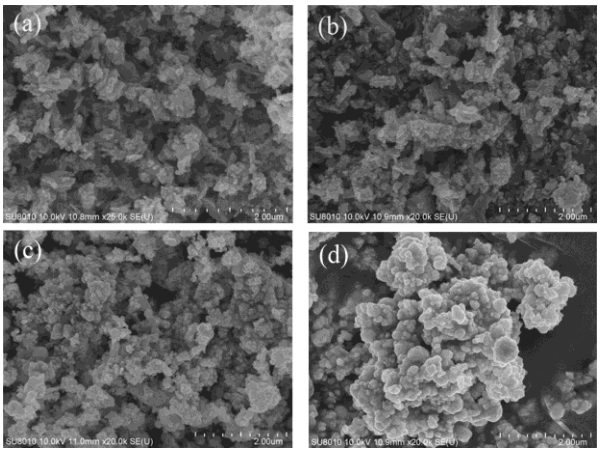

Fig. 2. FE-SEM images of pure ZnO and Cu/ZnO nanocomposites with different Cu concentration. (a) ZnO; (b) 20 wt% Cu; (c) 60 wt% Cu; (d) Cu

3.3 Optical characteristics

Fig. 3 shows the UV-vis absorption spectra of the samples measured between 250~800 nm. It is obvious

that the pure ZnO spectra show high transparency in the visible range and a sharp absorption edges appears at about 385 nm in the ultraviolet range, implying ZnO is a kind of UV-shielding material [18]. The optical absorption of Cu/ZnO nanocomposites were improved significantly in the visible range, and with the increase of Cu content, the absorption coefficient becomes higher. The band gap of the samples were calculate from the linear fit in the plot of $(\alpha hv)^2$ versus hv, where α is the absorption coefficient and hv is the photo energy. Then extrapolate of the linear portion of $(\alpha hv)^2$ to zero to get the band gap E_g of the samples [4]. As shown in Fig. 3 the band gap (E_g) of pure ZnO is 3.246 eV, and it decreases with the increase of Cu content.

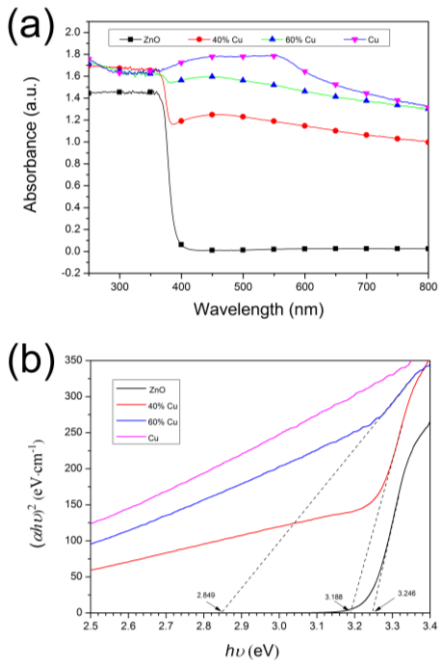

Fig. 3(a) UV-Vis absorption spectra and (b) determination of band gap energy for the samples

Fig. 4 (a) shows the variation of absorption spectra of MO aqueous solution in the presence of 60 wt% Cu/ZnO nanocomposites under visible light. It can be found that the characteristic absorbance peak of MO at 464 nm gradually decreases under visible light irradiation and the color of MO solution become lighter. Fig. 4(b) shows the degradation curves of MO using pure ZnO and Cu/ZnO nanocomposites with different Cu composition powders as photocatalysts under visible light irradiation. C_0 is the initial concentration of MO, C_t is the concentration of MO after t minutes. It can be seen that all the Cu/ZnO nanocomposities samples exhibit higher photocatalytic activities compared to the pure ZnO under visible light irradiation and the photocatalytic effect of the Cu/ZnO nanocomposities enhances gradually with the increase of Cu composition. However, the photocatalytic activity of the Cu/ZnO nanocomposities samples decrease with the increase of Cu content when the value exceeds 60%. Similar results were found by in the literature [19,20].

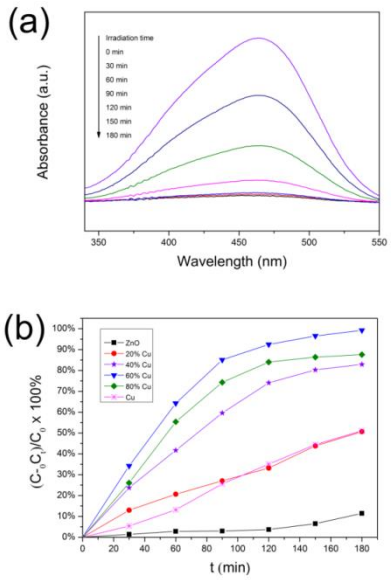

Fig. 4 (a) Absorption spectra of MO aqueous solution in the presence of 60 wt% Cu/ZnO nanocomposites; (b) Degradation curves of MO using pure ZnO and Cu/ZnO nanocomposites with different Cu composition powders as photocatalysts under visible light irradiation

Cu composition powders as photocatalysts under visible light irradiation. C_0 is the initial concentration of MO;C_t is the concentration of MO after t minutes. It can be seen that all the Cu/ZnO nanocomposities samples exhibit higher photocatalytic activities compared to the pure ZnO under visible light irradiation and the photocatalytic effect of the Cu/ZnO nanocomposities enhances gradually with the increase of Cu composition. However, the photocatalytic activity of the Cu/ZnO nanocomposities samples decrease with the increase of Cu content when the value exceeds 60 wt%. Similar results were found by in the literature [19,20].

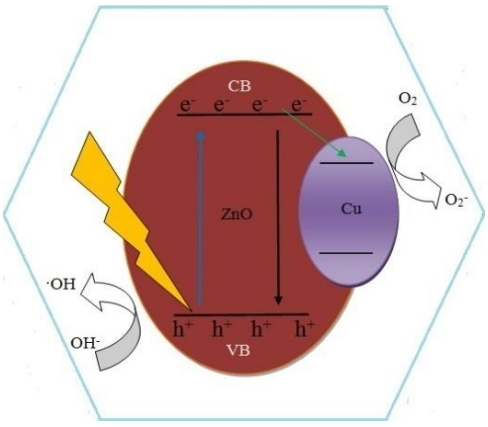

Fig. 5. Proposed mechanism for the photodegradation of MO by Cu/ZnO nanocomposites under visible light irradiation

According to the result we can infer that, when Cu nanoparticles were successfully deposited on the surface of ZnO, a new interaction was established between Cu and ZnO. The band gap (Eg) of the nanocomposites is lower than pure ZnO, which can be clear seen in Fig. 3 (b). In that case, the utilization rate of light is increased. When under irradiation, the electrons in the valence band (VB) of ZnO can be excited to the conduction band (CB) with simultaneous generating the same amount of holes when the photo energy of the illuminated UV light higher than the band gap of ZnO. The photoexcited electrons on the conduction band (CB) could transfer from ZnO to Cu nanoparticles. Therefore, Cu nanoparticles act as electron sinks. The recombination of photo-induced electron-holepairs can be inhibited efficiently. Therefore, the photocatalytic activity of the Cu/ZnO nanocomposites is highly improved under visible light irradiation. However, superfluous Cu particles deposited on the surface of ZnO will inhibit visible light irradiate to the interface of the Cu/ZnO. In addition, Cu particles also act as recombination centers at high Cu deposition which leads to the decrease of the photocatalytic performance. The ideal Cu content is 60 wt%.

4. Conclusion

Cu/ZnO nanocomposites were synthesized and Cu nanoparticles were successfully deposited on the surface of ZnO. The results revealed that the Cu/ZnO nanocomposites exhibited enhanced photocatalytic activity in degrading MO dyes compared with pure ZnO under visible light, which can be attributed to strong interaction between Cu and ZnO nanocrystals. Cu nanoparticle deposited on the surface of ZnO act as electron sinks to enhance the separation of photoexcited electrons from holes and also act as recombination centers at high Cu deposition which leads to the decrease of the material's photocatalytic activity. The 60 wt% Cu, ZnO samples presents the best photocatalytic activity.

Acknowledgements

We gratefully acknowledge funding from the National Natural Science Foundation of China (grant nos. 41402310 and 41472042). SFBSRCC (no. CUGL 150805), the Fundamental Research Founds for National University (grant nos. 1410491B04 and 1510491B01) and TLOF (grant nos. SKJ2013012 and SKJ2014035), China University of Geosciences (Wuhan).

References

[1] O. Carp, C. L. Huisman, A. Reller, Solid State Chem. **32**, 177 (2004).
[2] X. W. Duan, G. Z. Wang, H. Q. Wang, Y. Q. Wang, C. Shen, W. P. Cai, Cryst. Eng. Comm. **12**, 2821 (2010).
[3] C. G. Tian, Q. Zhang, B. J. Jiang, G. H. Tian, H. G. Fu, J. Alloys Compd. **509,** 6935 (2011).
[4] Y. Z. Zhang, L. H. Wu, H. Li, J. H. Xu, L. Z. Han, B. C. Wang, Z. L. Tuo, E. Q. Xie, J. Alloys Compd. **473**, 319 (2009).
[5] A. McLaren, T. Valdes-Solis, G. Q. Li, S. C. Tsang, J. Am. Chem. Soc. **131**, 12540 (2009).
[6] L. Wang, L. X. Chang, B. Zhao, G. Shao, W. Zheng, Inorg. Chem. **47**, 1443 (2008).
[7] Z. W. Deng, M. Chen, G. X. Gu, L. M. Wu, J. Phys. Chem. B **112**, 16 (2008).
[8] K. H. Tam, C. K. Cheung, Y. H. Leung, A. B. Djurišić, C. C. Ling, C. D. Beling, S. Fung, W. M. Kwok, W. K. Chan, D. L. Phillips, L. Ding, W. K. Ge, J. Phys. Chem. B **110**, 20856 (2006).
[9] B. P. Nenavathua, A. K. Rao, A. Goyal, A. Kapoor, R. K. Dutta, Appl. Catal. A **459**, 106 (2013).
[10] M. M. Ba-Abbad, A. A. H. Kadhum, A. B. Mohamad, M. S. Takriff, K. Sopian, Chemosphere **91**, 1604 (2013).
[11] H. B. Lu, H. Li, L. Liao, Y. Tian, M. Shuai, J. C. Li, M. F. Hu, Q. Fu, B. P. Zhu, Nanotechnology **19**, 145605 (2008).
[12] M. Ahmad, E. Ahmed, Z. L. Hong, N. R. Khalid, W. Ahmed, A. Elhissi, J. Alloys Compd. **577**, 717 (2013).
[13] H. Gu, Y. Yang, J. X. Tian, G. Y. Shi, Appl. Mater. Interfaces **5**, 6762 (2013).
[14] Y. Y. Zhang, J. Mu, J. Colloid Interf. Sci. **309**, 478 (2007).
[15] P. Pawinrat, O. Mekasuwandumrong, J. Panpranot, J. Catal. Commun. **10**, 1380 (2009).
[16] Y. G. Chang, J. Xu, Y. Y. Zhang, S. Y. Ma, L. H. Xin, L. N. Zhu, C. T. Xu, J. Phys. Chem. C **113**, 18761 (2009).
[17] O. Deng, X. W. Duan, D. H. L. Ng, H. B. Tang, Y. Yang, M. G. Kong, Z. K. Wu, W. P. Cai, G. Z. Wang, Appl. Mater. Interfaces. **4**, 6030 (2012).
[18] Y. Q. Li, S. Y. Fu, Y. W. Mai, Polymer **47**, 2127 (2006).
[19] Y. H. Zheng, C. Q. Chen, Y. Y. Zhan, X. Y. Lin, Q. Zheng, K. M. Wei, J. F. Zhu, J. Phys. Chem. C **112**, 10773 (2008).
[20] Y. H. Zheng, L. R. Zheng, Y. Y. Zhan, X. Y. Lin, Q. Zheng, K. M. Wei, Inorg. Chem. **46**, 6980 (2007).

*Corresponding author: liuchangzhen@163.com
xlwu@cug.edu.cn